Biocompatible Alkyne arms containing Schiff base Fluorescence Indicator for Duel detection of Cd^{II} and Pb^{II} at Physiological pH and its Application to Live Cell Imaging

S.G. Jebastin Andrews,[†] S. Benita Jeba Silviya,[†] Dharmaraj Jeyanthi,[†] E. Sathya Devi,[†] J. Winfred Jebaraj,[§] and Chithiraivel Balakrishnan[*,†]

[†]Department of Chemistry, Nazareth Margoschis College at Pillaiyanmanai, Nazareth - 628 617, Thoothukudi District, Tamil Nadu, India

[§]Department of Chemistry, St.John's College, Palayamkottai, Tirunelveli, Tamilnadu, India

*Corresponding Author

Tel: +91 7845061380

E-mail: balac0735@gmail.com; pcvelbala@gmail.com

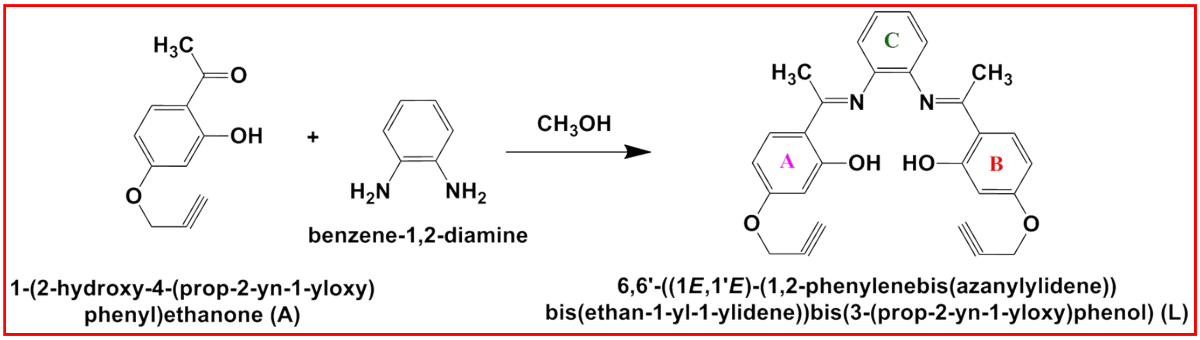

Scheme S1. Synthetic scheme for L.

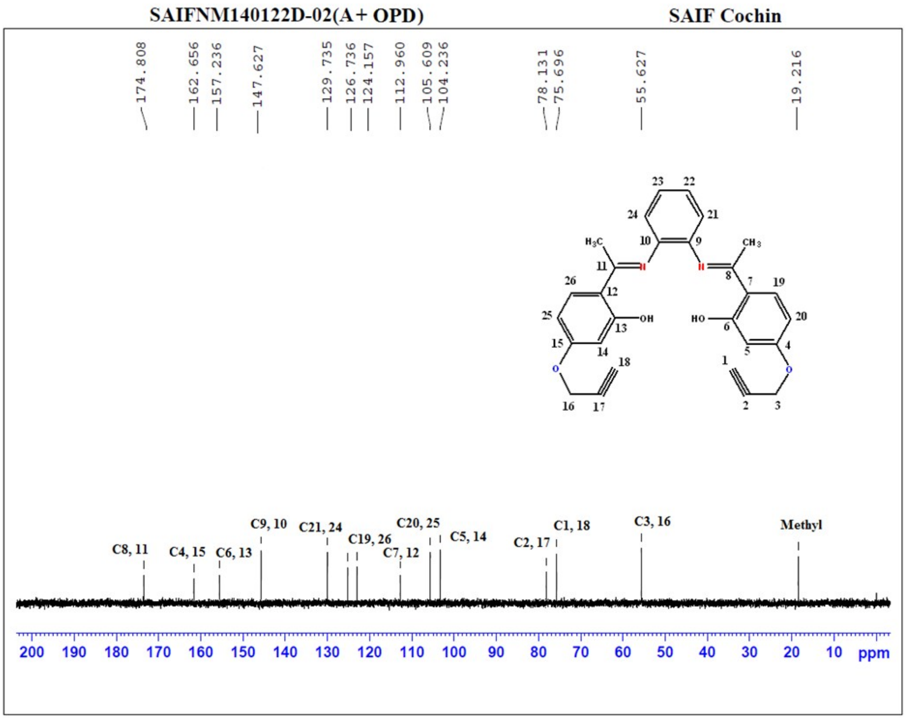

Fig. S1.^{13}C NMR spectrum of H_2L.

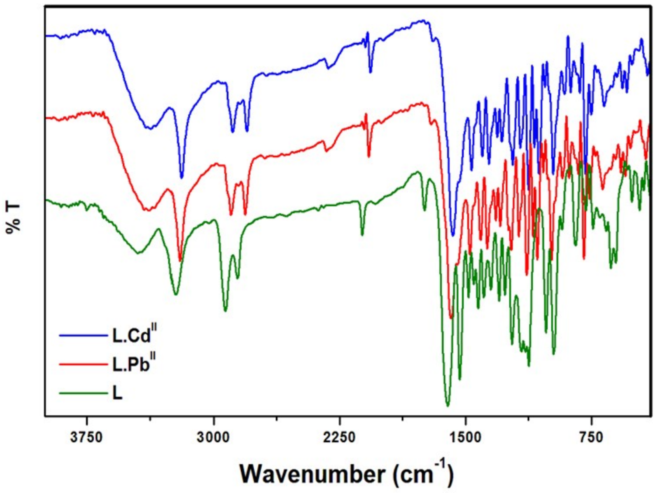

Fig. S2.FT-IR spectra of H_2L and its complexes, L.Cd^{II} and L.Pb^{II})

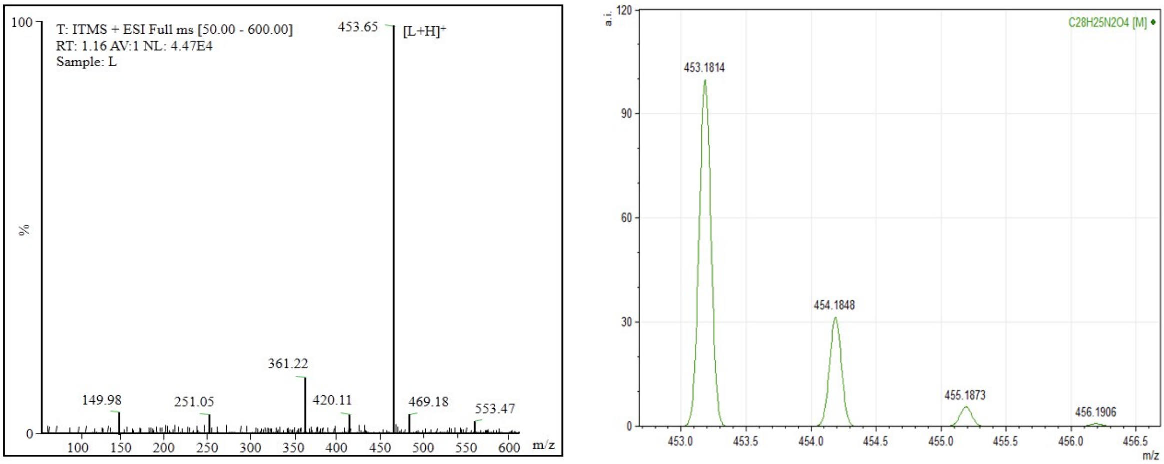

(a) **(b)**

Fig. S3.ESI-mass spectra of compound H_2L, **(a)** experimental; **(b)** simulated.

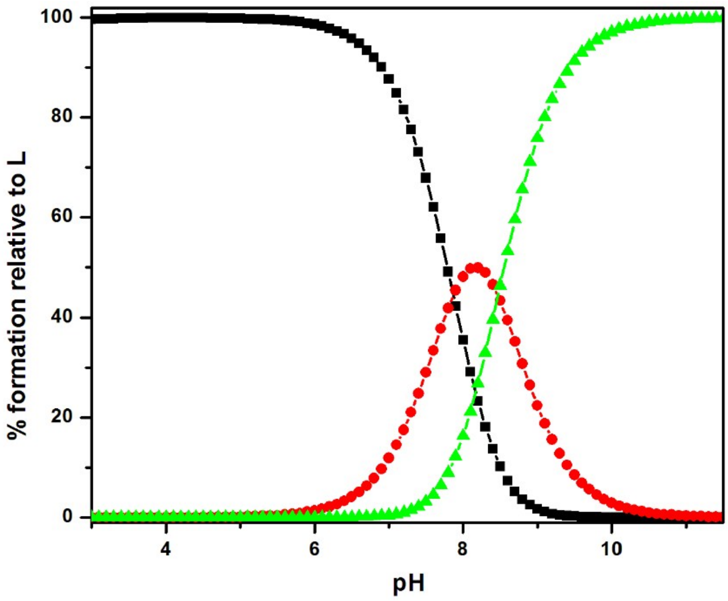

Fig.S4. Protonation equilibria diagram of H_2L (C_L = 0.003 M) in methanol/HEPES buffer (5 mM, pH 7.3; 1:9 v/v).

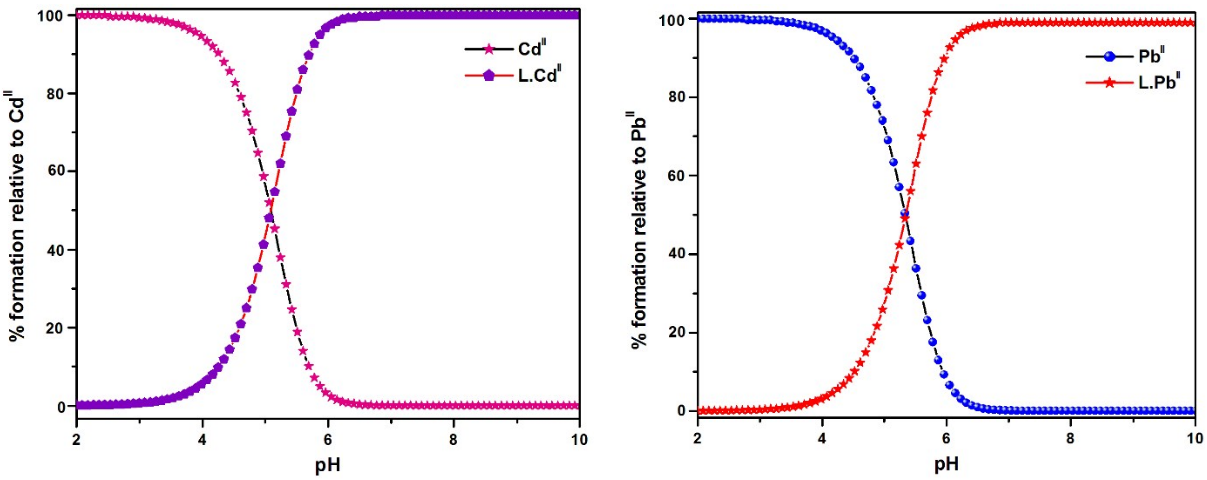

(a) **(b)**

Fig. S5. Species distribution diagram of (a) L.Cd^{II} and (b) L.Pb^{II} complex equilibria in methanol/HEPES buffer (5 mM, pH 7.3; 1:9 v/v).

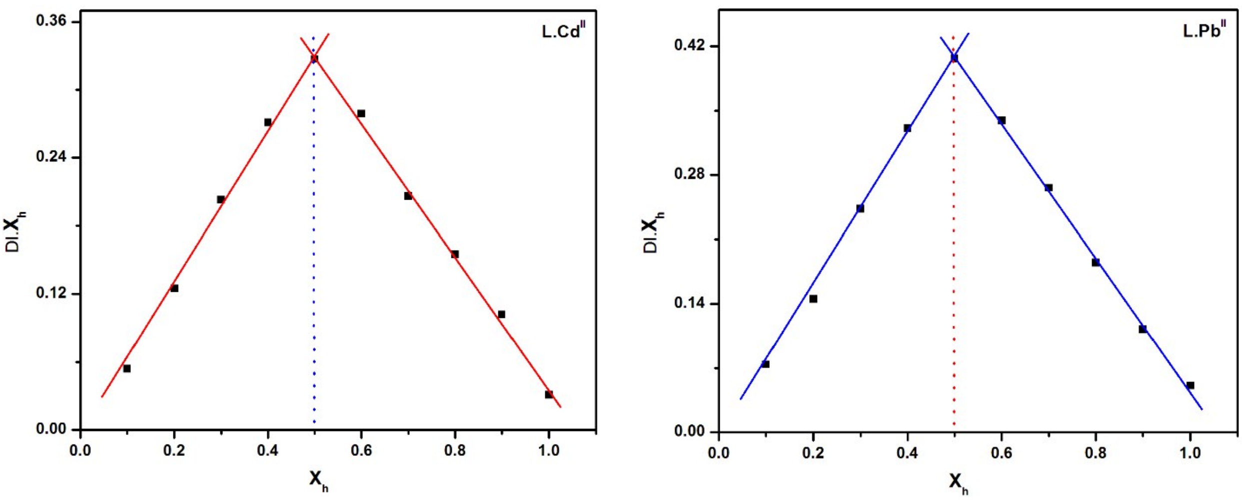

(a) **(b)**

Fig. S6. Job's plot analysis H_2L with **(a)** Cd^{II} and **(b)** Pb^{II}.

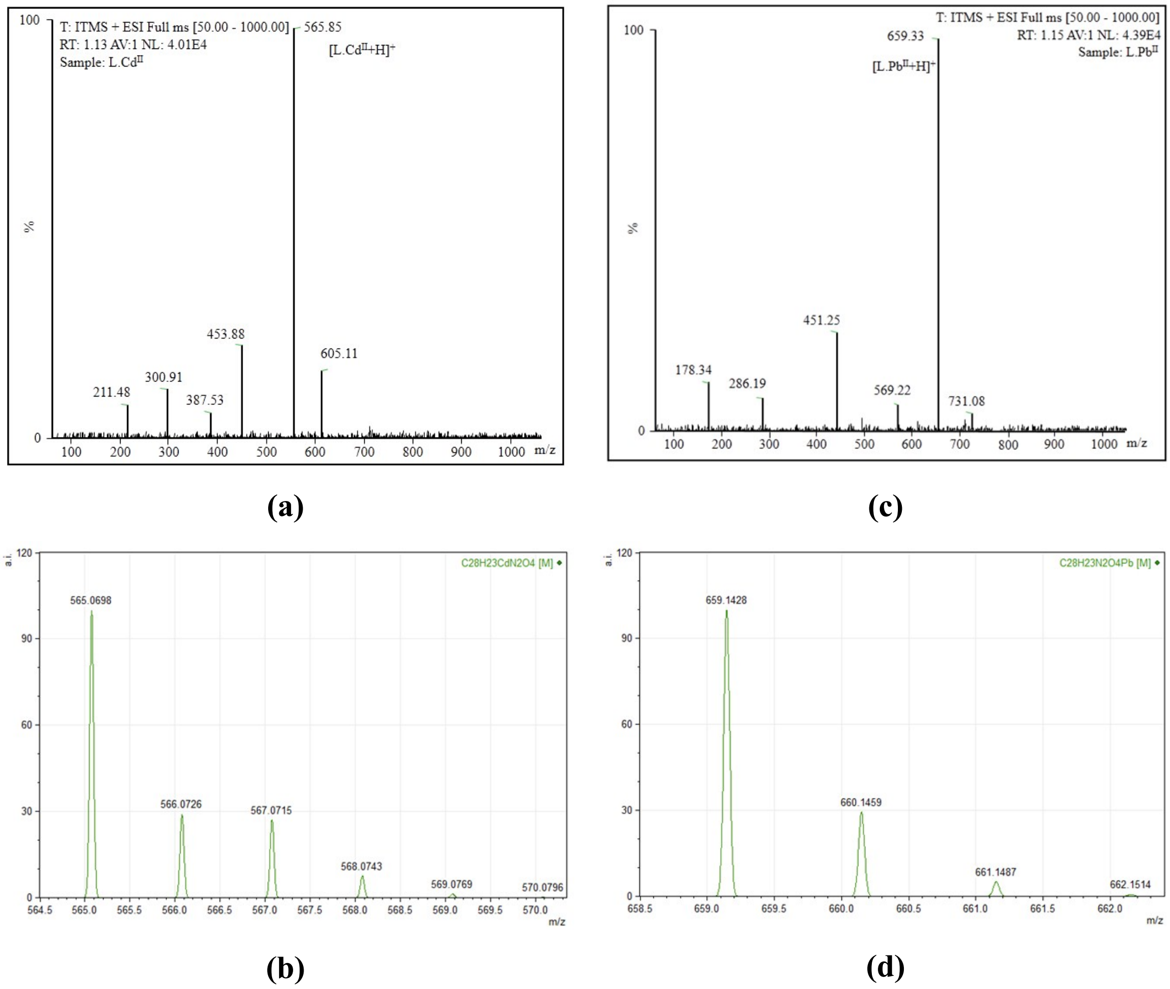

Fig. S7.ESI-mass spectra of **(a)** experimental L.Cd^{II}; **(b)** simulated L.Cd^{II}; **(c)** experimental L.Pb^{II} and **(d)** simulated L.Pb^{II}.

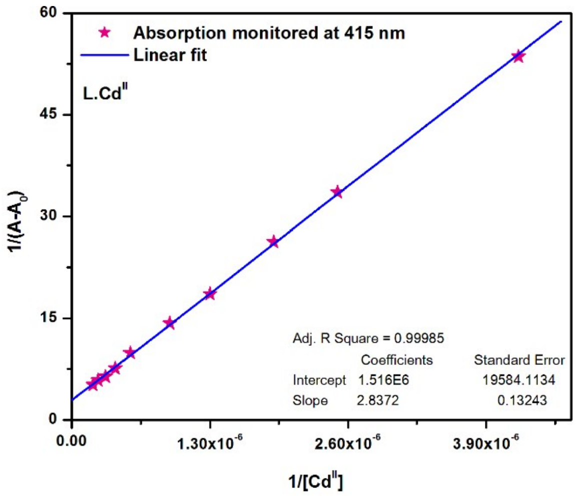

(a)

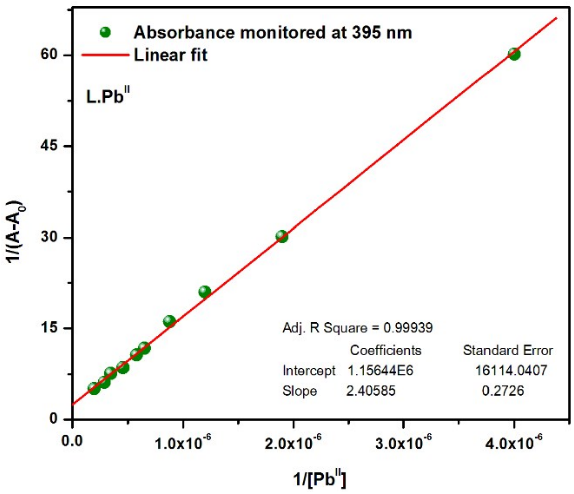

(b)

Fig.S8. B-H plot from absorption titration data of with **(a)** Cd^{II} and **(b)** Pb^{II} concentration.

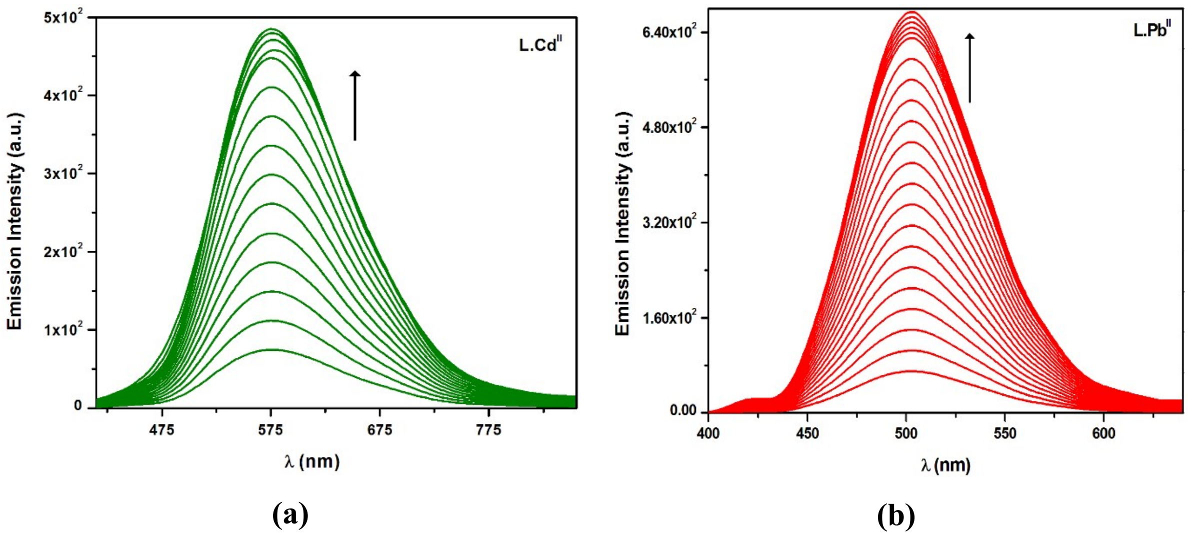

Fig. S9. Emission spectra of H_2L (10 μM) upon incremental addition of (a) Cd^{II} (0.0 – 5.0 equiv.) and (b) Pb^{II} (0.0 – 5.0 equiv.) in methanol/HEPES buffer (5 mM, pH 7.3; 1:9 v/v).

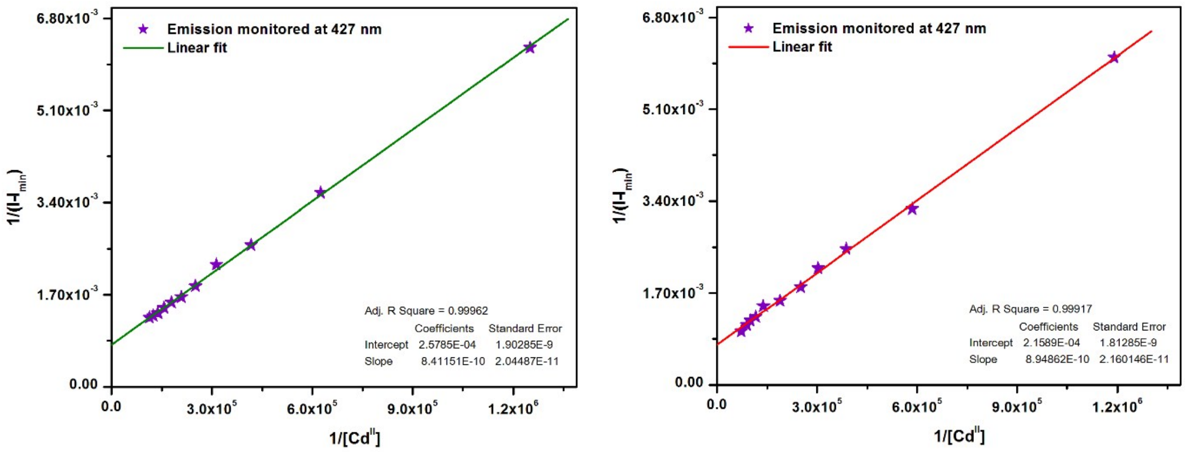

(a) **(b)**

Fig. S10. B-H plot from emission titration data of with **(a)** Cd^{II} and **(b)** Pb^{II} concentration.

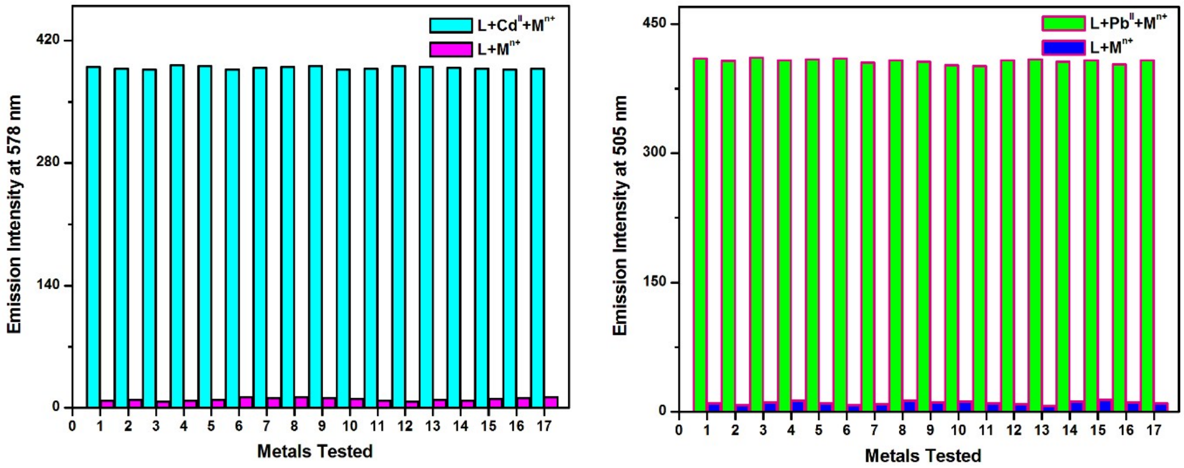

(a) **(b)**

Fig.S11. Emission intensity of H_2L (10 μM) with **(a)** Cd^{II} in the presence of other metal ions in methanol/HEPES buffer (5 mM, pH 7.3; 1:9 v/v) at room temperature. (1) $L+Cd^{II}+Ag^{I}$, (2) $L+Cd^{II}+Zn^{II}$, (3) $L+Cd^{II}+Al^{III}$, (4) $L+Cd^{II}+Pb^{II}$, (5) $L+Cd^{II}+Mn^{II}$, (6) $L+Cd^{II}+Hg^{II}$, (7) $L+Cd^{II}+Mg^{II}$, (8) $L+Cd^{II}+Cu^{II}$, (9) $L+Cd^{II}+Fe^{II}$, (10) $L+Cd^{II}+Fe^{II}$, (11) $L+Cd^{II}+Co^{II}$, (12) $L+Cd^{II}+Ni^{II}$, (13) $L+Cd^{II}+Na^{I}$, (14) $L+Cd^{II}+VO^{II}$, (15) $L+Cd^{II}+Mn^{II}$, (16) $L+Cd^{II}+K^{I}$, (17) $L+Cd^{II}+Ca^{II}$ and **(b)** Pb^{II} in the presence of other metal ions in methanol/HEPES buffer (5 mM, pH 7.3; 1:9 v/v) at room temperature. (1) $L+Pb^{II}+Ag^{I}$, (2) $L+Pb^{II}+Zn^{II}$, (3) $L+Pb^{II}+Al^{III}$, (4) $L+Pb^{II}+Cd^{II}$, (5) $L+Pb^{II}+Mn^{II}$, (6) $L+Pb^{II}+Hg^{II}$, (7) $L+Pb^{II}+Mg^{II}$, (8) $L+Pb^{II}+Cu^{II}$, (9) $L+Pb^{II}+Fe^{II}$, (10) $L+Pb^{II}+Fe^{II}$, (11) $L+Pb^{II}+Co^{II}$, (12) $L+Pb^{II}+Ni^{II}$, (13) $L+Pb^{II}+Na^{I}$, (14) $L+Pb^{II}+VO^{II}$, (15) $L+Pb^{II}+Mn^{II}$, (16) $L+Pb^{II}+K^{I}$, (17) $L+Pb^{II}+Ca^{II}$.

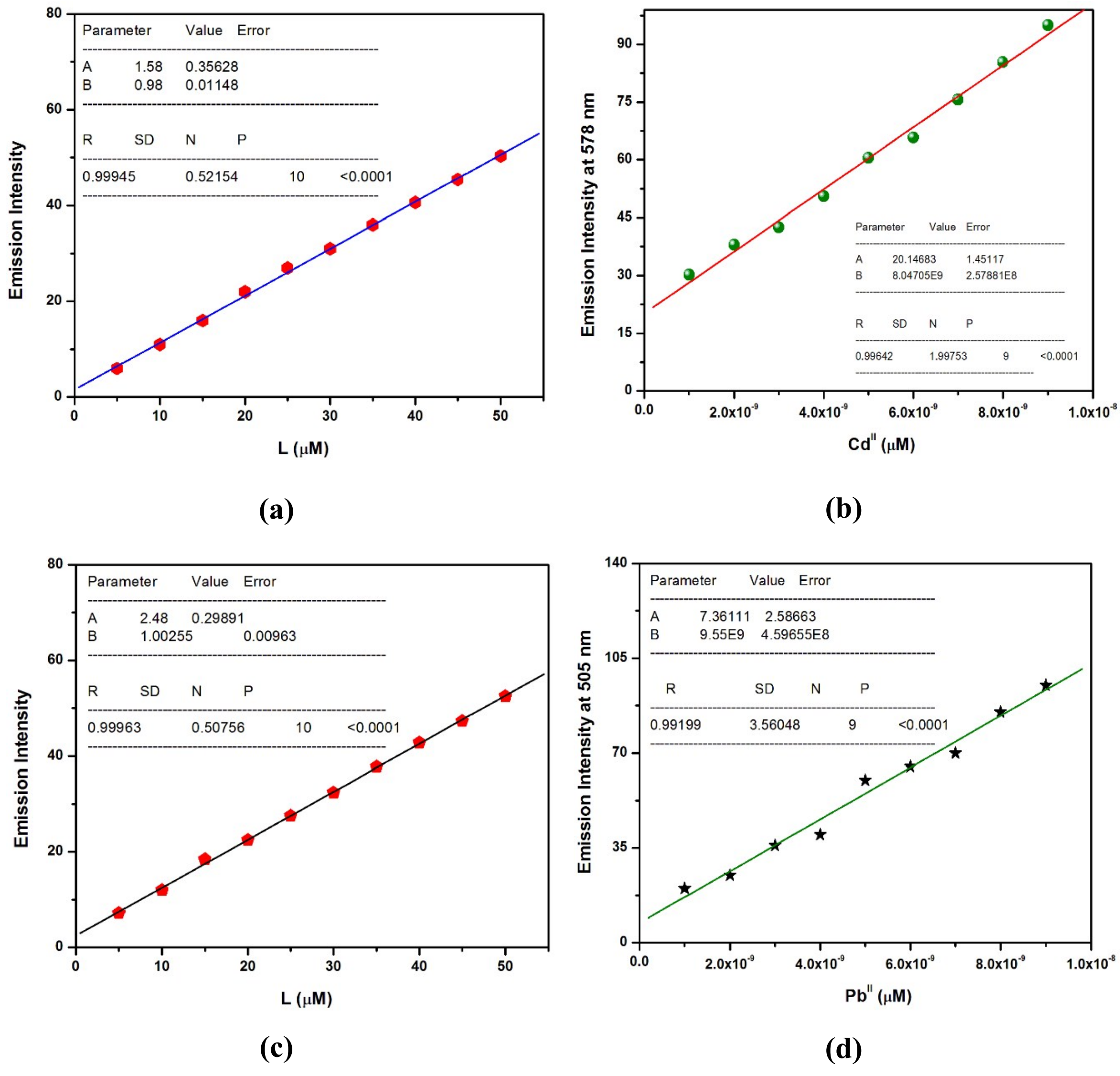

(a) (b) (c) (d)

Fig. S12. **(a)** Determination of Sb1 of the blank, H_2L solution; **(b)** Linear dynamic plot of emission intensity (at 578 nm) vs. [Cd^{II}] for the determination of S (slope) and **(c)** Determination of Sb1 of the blank, H_2L solution; **(d)** Linear dynamic plot of emission intensity (at 505 nm) vs. [Pb^{II}] for the determination of S (slope); [H_2L] = 10 μM.

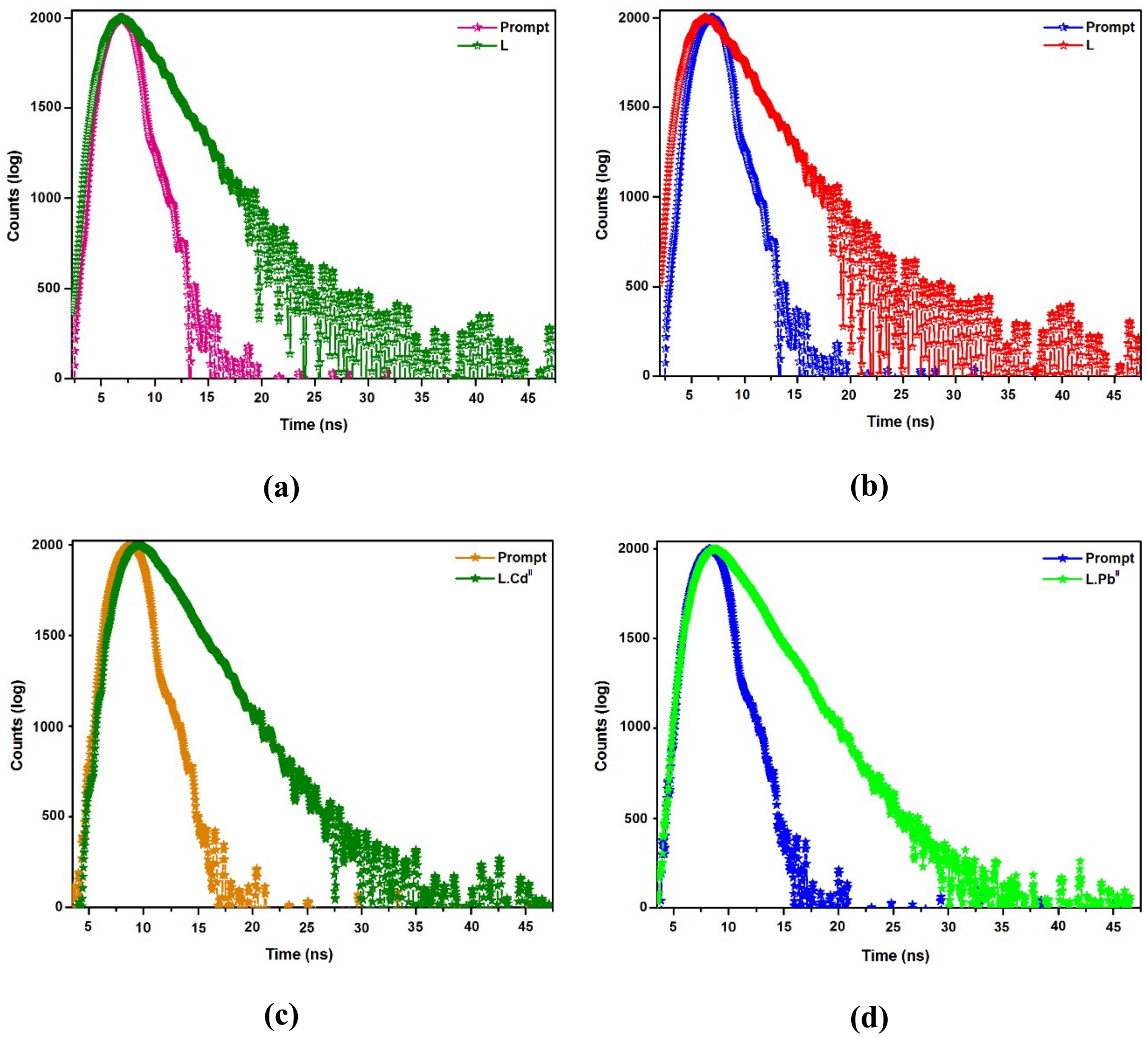

Fig. S13. Time-resolved fluorescence decay of **(a)** H_2L (10 μM; λ_{ex} = 420 nm); **(b)** H_2L (10 μM; λ_{ex} = 410 nm); **(c)** in presence of Cd^{II} metal ions (5 equiv.; λ_{ex} = 420 nm) and **(d)** in presence of Pb^{II} metal ions (5 equiv.; λ_{ex} = 410 nm) in acetonitrile/HEPES buffer (5 mM, pH 7.3; 1:9 v/v) at room temperature.

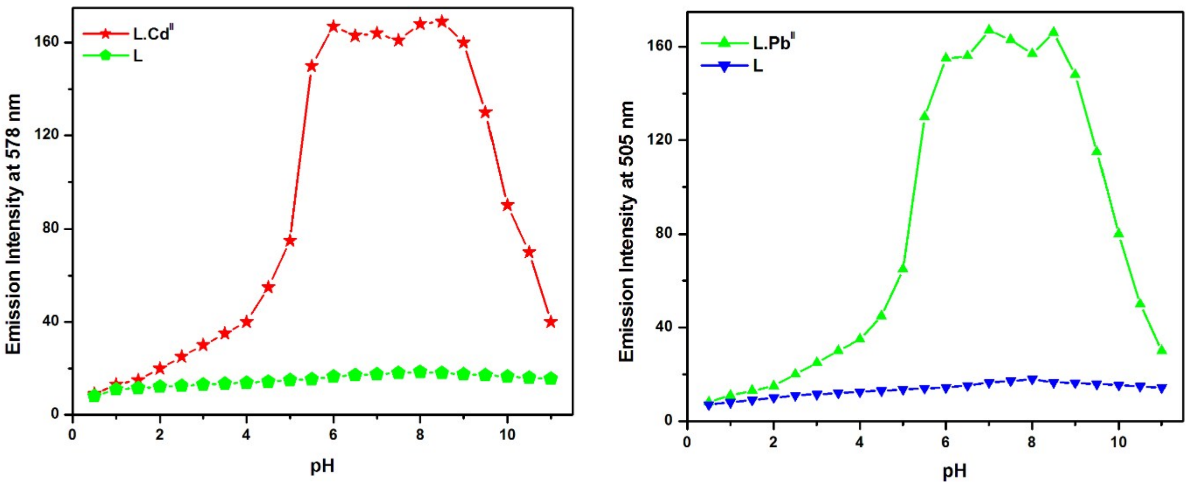

(a) **(b)**

Fig. S14. Emission intensity of H_2L in the presence of **(a)** Cd^{II} (λ_{em} = 578 nm; λ_{ex} = 420 nm); **(b)** Pb^{II} (λ_{em} = 505 nm; λ_{ex} = 410 nm) at various pH values in methanol/HEPES buffer (5 mM, pH 7.3; 1:9 v/v).

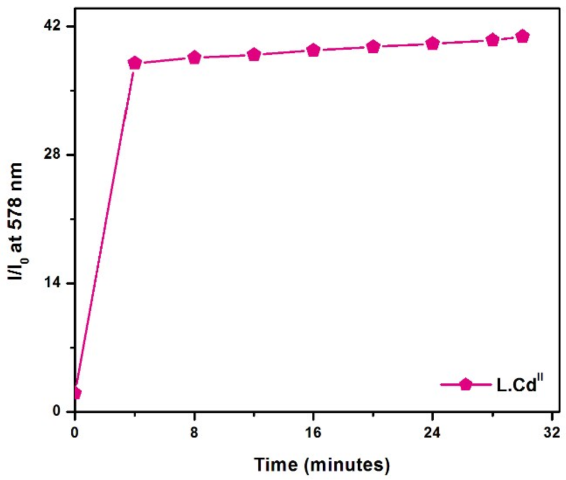

(a)

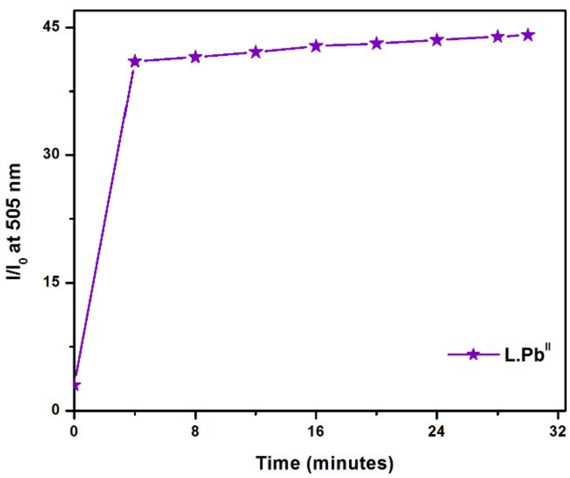

(b)

Fig. S15. Fluorescence intensity of **(a)** L.Cd^{II}; **(b)** L.Pb^{II} as a function of time (0-30 minutes).

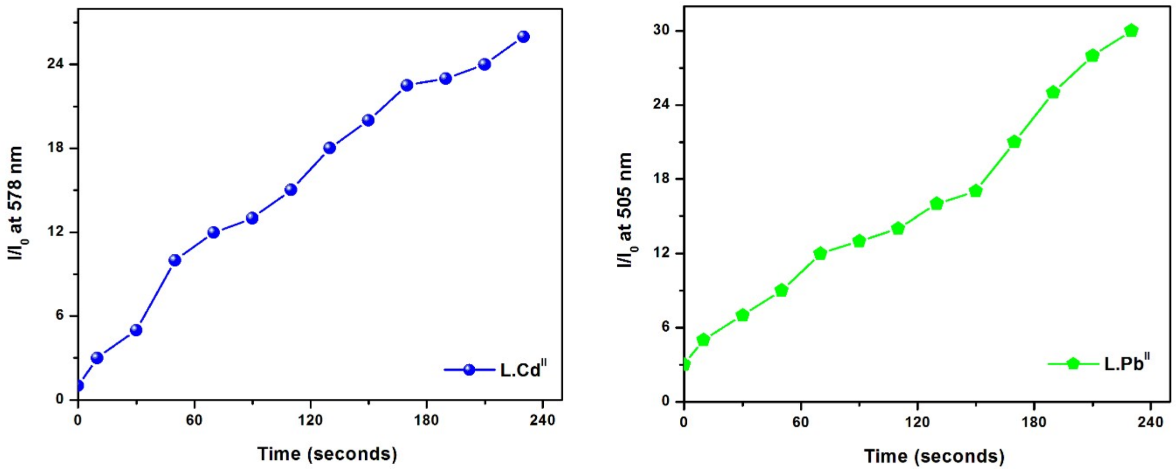

(a) **(b)**

Fig. S16. Emission intensity of **(a)** L.Cd^{II}; **(b)** L.Pb^{II} as a function of time (seconds).

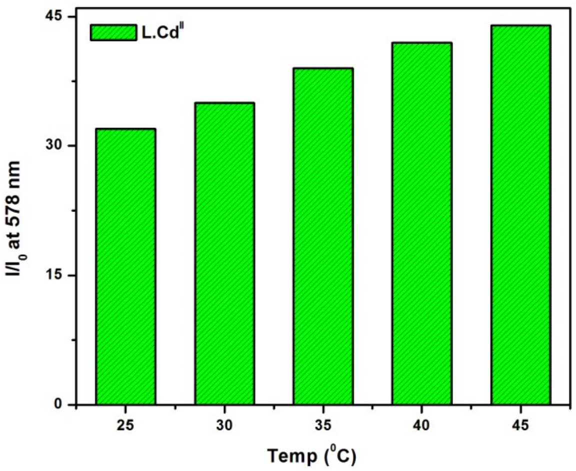

(a)

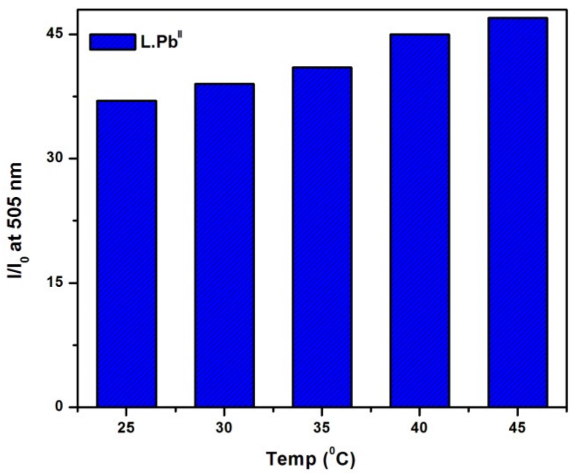

(b)

Fig. S17. Emission spectral changes of **(a)** L.Cd^{II}; **(b)** L.Pb^{II} as a function of temperature (25-45˚C).

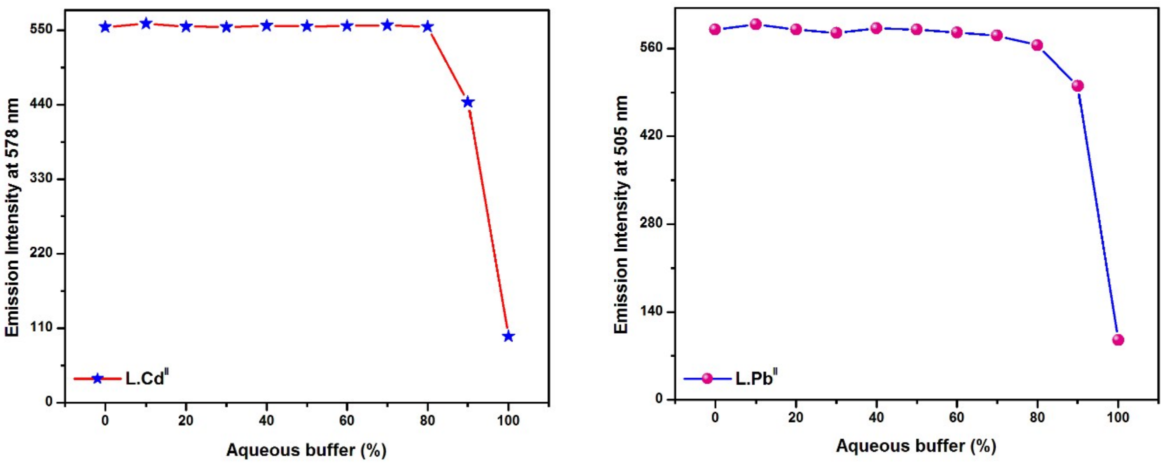

(a) **(b)**

Fig. S18. Fluorescence intensity of **(a)** L.Cd^{II}; **(b)** L.Pb^{II} as a function of aqueous buffer concentration (0-99%).

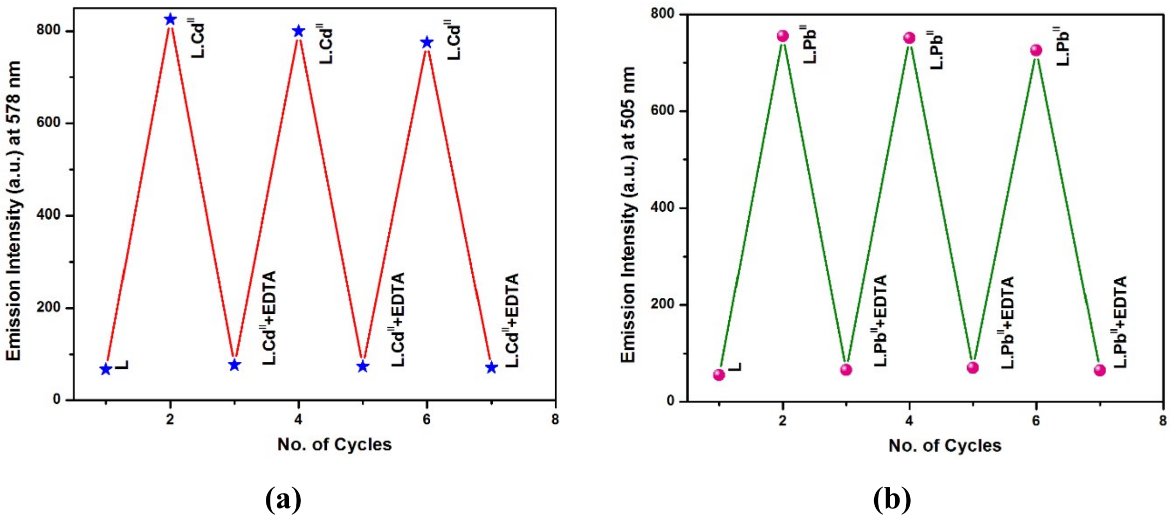

Fig. S19. (a) Emission intensities of L.Cd^{II} (1:1) in the presence of EDTA for many cycles (λ_{ex} = 420 nm; λ_{em} = 578 nm); (b) Emission intensities of L.Pb^{II} (1:1) in the presence of EDTA for many cycles (λ_{ex} = 410 nm; λ_{em} = 505 nm).

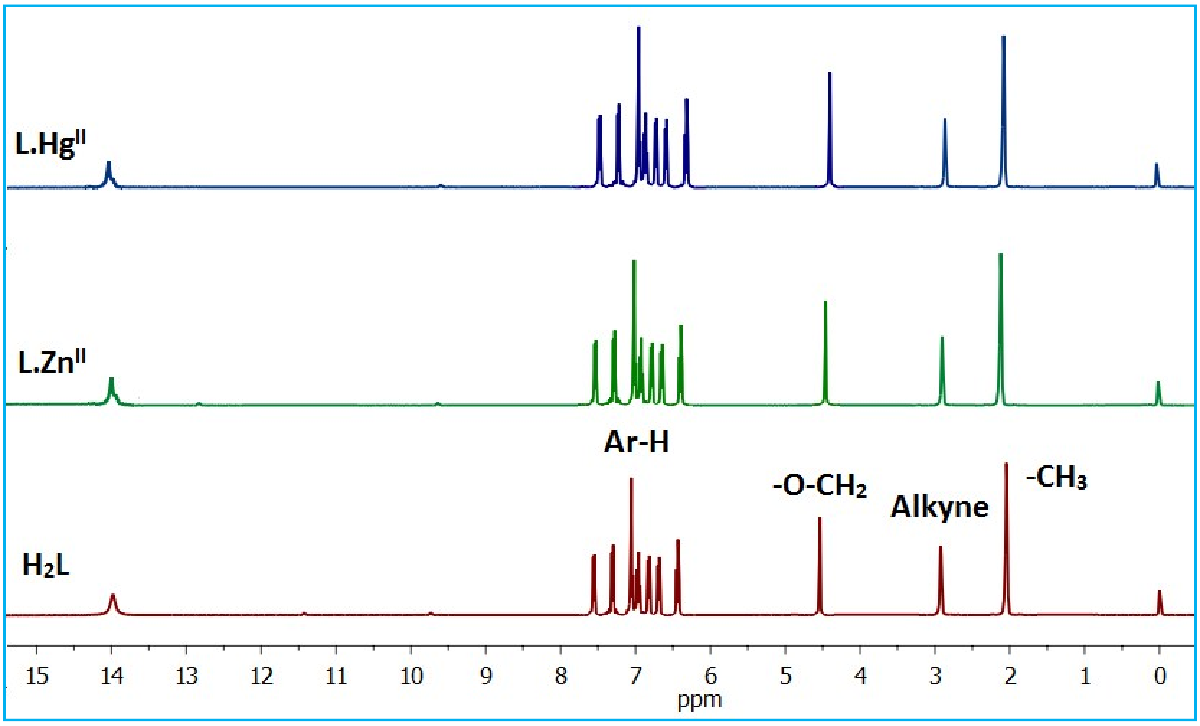

Fig. S20. ^{1}H NMR spectra of H_2L in the absence and presence of Zn^{II} and Hg^{II} ions in DMSO-d_6.

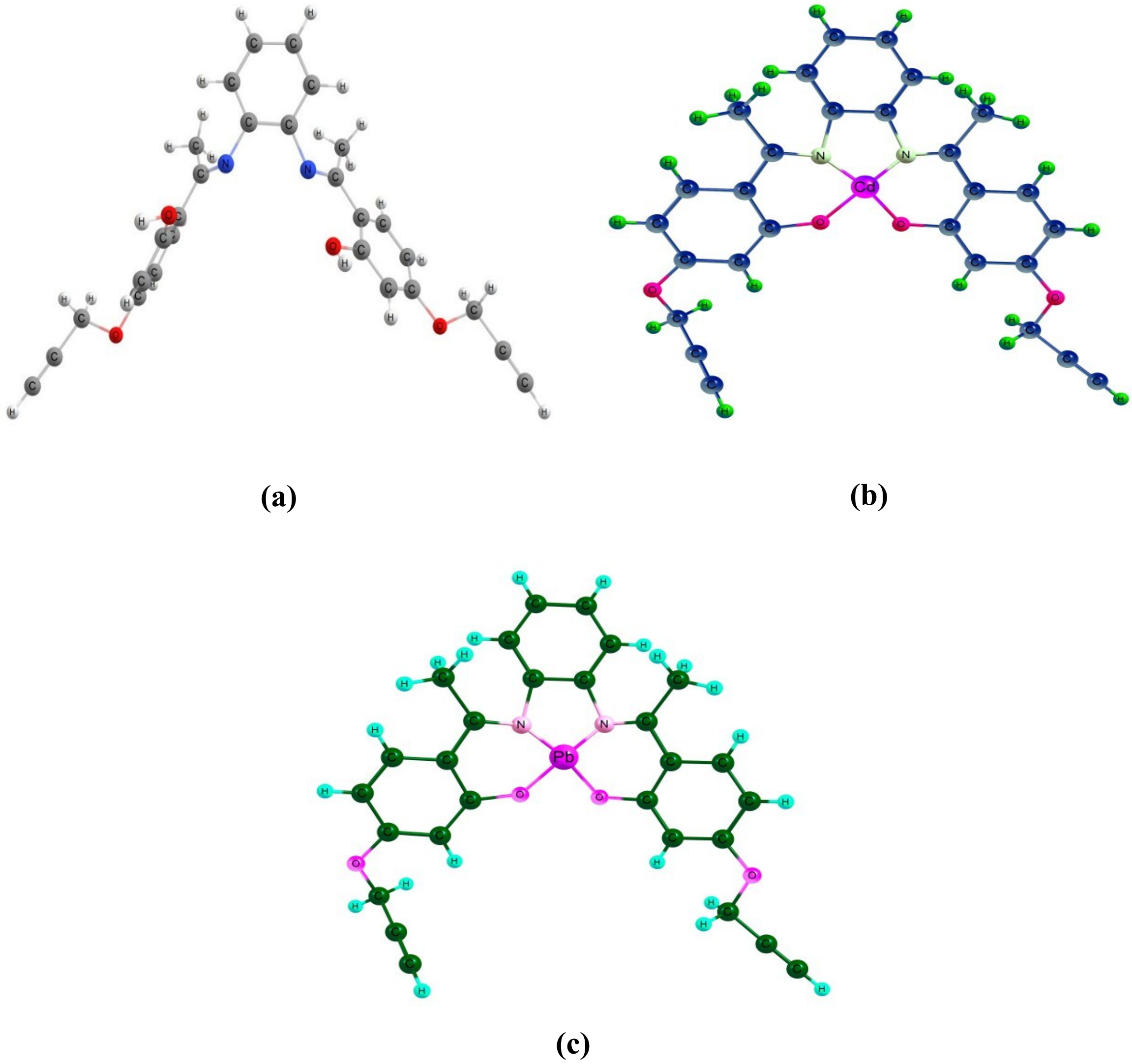

Fig. S21. Optimized geometry of **(a)** H_2L; **(b)** L.Cd^{II} and **(c)** L.Pb^{II} using Gaussian 16 at B3LYP/6-311G(d,p) level of theory.

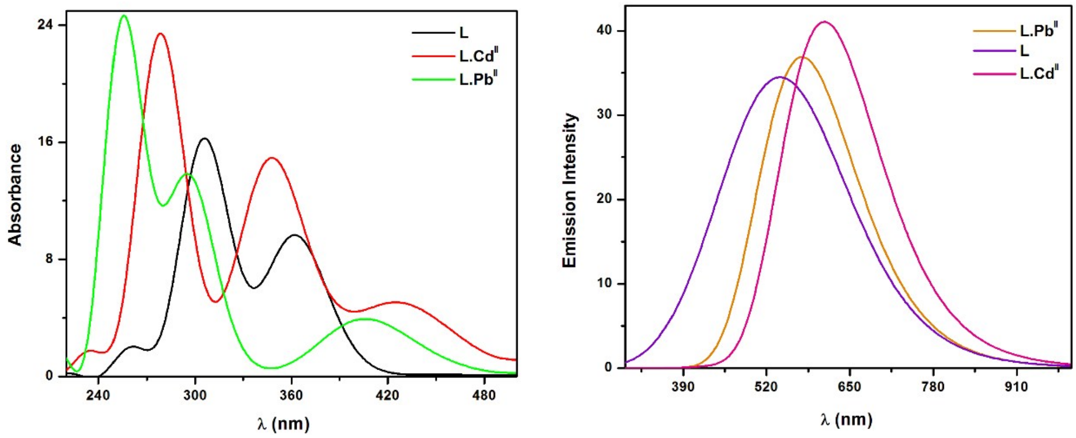

(a) **(b)**

Fig. S22. **(a)** Absorption and **(b)** emission spectra for H_2L with metal ions in the DFT method.

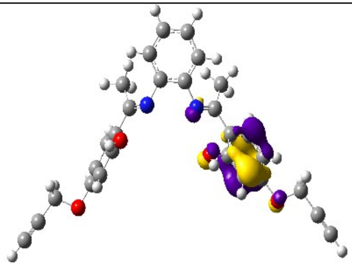	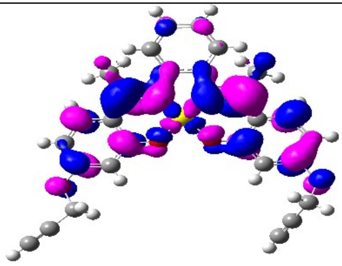	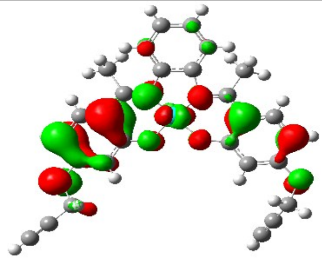
LUMO = -3.0245 (eV)	LUMO = -1.9947 (eV)	LUMO = -1.8114 (eV)
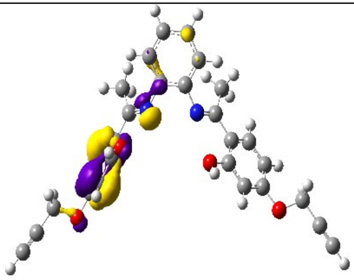	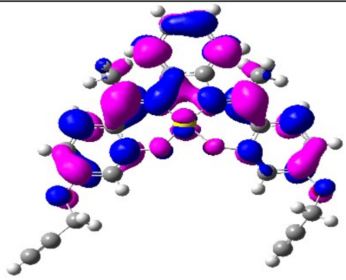	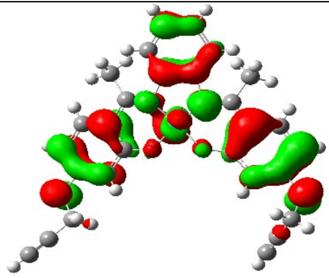
HOMO = -6.0543 (eV)	HOMO = -3.6534 (eV)	HOMO = -3.1354 (eV)
ΔE = 3.03 (eV)	ΔE = 1.66 (eV)	ΔE = 1.32 (eV)
(a)	**(b)**	**(c)**

Fig. S23.FMO diagrams of **(a)** H_2L; **(b)** L.Pb^{II} and **(c)** L.Cd^{II} with energy gap as calculated from the DFT method.

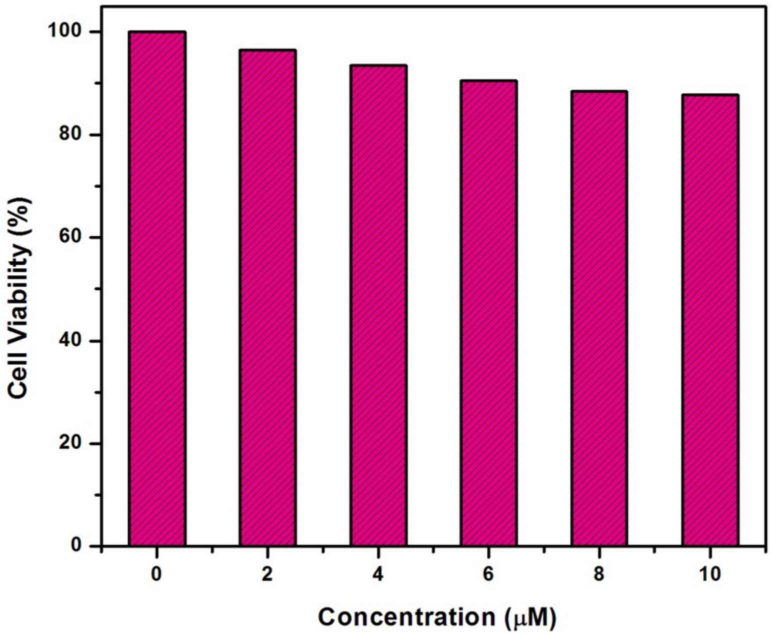

Fig. S24. Cell viability values (%) assessed by MTT proliferation test versus concentrations of H_2L after 24 h incubation at 25°C.

Binding of H_2L with Cd^{II} and Pb^{II}

a) By absorbance method

The $L.M^{II}$ (M = Cd and Pb) binding constant was measured using the Benesi-Hildebrand (B-H) plot.[S1]

$$1/(A - A_0) = a/(a - b)\{1/K_a[M] + 1 \ldots\ldots\ldots\ldots(1)$$

where A_0 is absorbance of free L, A is absorbance of H_2L with metal ions, K_a is the binding constant (M^{-1}) and [M] is the concentration of metal ions added during titration. The association constant (K_a) could be determined from the slope of the straight line of the plot of $1/(A - A_0)$ vs. $[1/M^{II}]$ and is found to be 5.30×10^5 M^{-1} ($L.Cd^{II}$) and 4.80×10^5 M^{-1} ($L.Pb^{II}$).

b) By fluorescence method

Also the binding constant value of metal ions with H_2L has been examined by fluorescence spectroscopic method using the modified Benesi-Hildebrand equation,

$$1/(I - I_0) = 1/\{K(I_{max} - I_0)C\}+1/(I_{max} - I_0) \ldots\ldots\ldots\ldots\ldots\ldots\ldots(2)$$

where I_0 is the emission intensity of H_2L in the absence of metal ions, I is the observed emission intensity at that particular wavelength in the presence of a certain concentration of the metal ion (C), I_{max} is the maximum fluorescence intensity value that was obtained during the titration with varying metal ion concentration, K is the binding constant (M^{-1}) and was determined from the slope of the linear plot and C is the concentration of the metal ions added during titration and is found to be 3.10×10^5 M^{-1} ($L.Cd^{II}$) and 2.40×10^5 M^{-1} ($L.Pb^{II}$).

Job Plot Method

The compound, H_2L (0.01M) was dissolved in methanol/HEPES buffer (5 mM, pH 7.3; 1:9v/v). 100, 90, 80, 70, 60, 50, 40, 30, 20, 10 and 0 µL of the solution of H_2L were taken and transferred to 5.0 ml bottles. Every bottle was diluted with water to make a total volume of 4.0 ml. Metal ions (0.01M) were dissolved in water. 0, 10, 20, 30, 40, 50, 60, 70, 80, 90 and 100 µL of the metal ion solution were added to each diluted solution of H_2L. Each bottle had a total volume of 5.0 ml. After shaking them for 5 minutes, absorption spectra were taken at room temperature. Job's plots were drawn by plotting $\Delta I.X_h$ vs. X_h, where ΔI = change of absorbance at 349 nm during titration and X_h is the mole fraction of metal ions).

pH Study

The pH titrations were done in an automatic potentiometric titrator (HANNA-HI-902, USA) at 310 K with a combined glass electrode (accuracy ± 0.01 pH unit). The instrument was calibrated using standard buffer solutions.[S2] The ionic strength of each solution was adjusted to 0.10 M with $NaClO_4$ as the supporting electrolyte. The ion product of water ($K = [H^+][OH^-]$) at 0.10 M $NaClO_4$ in methanol/HEPES buffer (5 mM, pH 7.3; 1:9 v/v) mixture was calculated based on the measurement of $[H^+]$ and $[OH^-]$ and pH in several experiments. The nitrogen gas was bubbled through the solution before and during titrations. Multiple titrations were carried out for each system. The dissociation constants (pK_a) of H_2L were obtained from its solutions of concentration ranging from 1.0×10^{-3} to 3.0×10^{-3} M. The pKa values were calculated with the help of the MINIQUAD-75 program. The concentration distribution profiles were obtained[S3] with HYSS.

Determination of quantum yield

The fluorescence quantum yield (Φ_x) for H_2L and L.M^{II} (M = Cd and Pb) was measured at room temperature using standard solutions of fluorescein $(\Phi_x = 0.79)$ in basic methanol at an excitation wavelength 441 nm. The quantum yield was determined by the following eqn,

$$\Phi_x = \Phi_{st} \bullet (A_{st}/A_x) \bullet (F_x/F_{st}) \bullet (n_x^2/n_{st}^2) \bullet (D_x/D_{st})$$

where, Φ_x is the quantum yield of the sample, Φ_{st} is the quantum yield of the reference, $A_x$and A_{st} are the absorbances of the sample and the reference, F_x and $F_{st}$are the areas of emission for the sample and the reference, n_x^2 and n_{st}^2 are the refractive indexes of the solvents and D_x and $D_{st})$ is the dilution factor of the sample and reference respectively.

Calculation:

For Cd^{II}

Φ_{st} = 0.79, A_{st} = 441 nm, A_x = 415 nm, F_x = 65452.2, F_{st} = 204536.6, (n) = 1.3335, D_x = 0.002 and D_{st} = 0.003

$$\Phi_x = 0.79 \bullet (441/415) \bullet (65452.2/204536.6) \bullet (1.3335/1.3335) \bullet (0.002/0.003)$$

$$\Phi_x = 0.2869$$

For Pb^{II}

Φ_{st} = 0.79, A_{st} = 441 nm, A_x = 405 nm, F_x = 63541.2, F_{st} = 197825.6, (n) = 1.3349, D_x = 0.002 and D_{st} = 0.003

$$\Phi_x = 0.79 \bullet (441/405) \bullet (63541.2/197825.6) \bullet (1.3349/1.3349) \bullet (0.002/0.003)$$

$$\Phi_x = 0.1842$$

For H_2L

Φ_{st} = 0.79, A_{st} = 441 nm, A_x = 349 nm, F_x = 25122.7, F_{st} = 189874.8, (n) = 1.3252, D_x = 0.002 and D_{st} = 0.003

$$\Phi_x = 0.79 \bullet (441/349) \bullet (25122.7/189874.8) \bullet (1.3252/1.3252) \bullet (0.002/0.003)$$

$$\Phi_x = 0.0880$$

Reversibility Test

The reversible performance of proposed sensor has been proving with EDTA disodium salt. The ligand, L (10 μM) was dissolved in methanol (1.0 mL) and 4.0 ml of the metal ion solution mixed with 1.0 mL solution of L. After mixing it for 2 minutes, the fluorescence spectra were taken at room temperature. EDTA (0.5 mmol) was dissolved in 5.0 ml of water and 2.0 mL of the EDTA solution were added to the solution of the $L.M^{II}$ (M = Cd and Pb) complex. After mixing it for 2 minutes, fluorescence spectra were taken at room temperature. The disodium salt of EDTA is a heavy metal ion chelator, leads to quenching the emission intensity of $L.M^{II}$ complex, indicating that L reversibly coordinates to metal ions.

Table S1. Emission lifetime of H_2L (10 μM) and its complexes Cd^{II} and Pb^{II} ion in acetonitrile/HEPES buffer (5 mM, pH 7.3; 1:9 v/v)

	τ (ns)	χ^2
H_2L (420 nm)	7.54	1.09815
H_2L (410 nm)	5.99	1.07124
$L.Cd^{II}$ (420 nm)	9.67	1.11829
$L.Pb^{II}$ (410 nm)	8.85	1.10911

Table S2. Comparison of λ_{abs} and λ_{em} of the metal complex along with oscillator strength as observed in experimental and theoretical calculations.

	Experimental (nm)	**Theoretical (nm)**	**Oscillator strength (*f*)**
Absorption			
H_2L	266, 349	320, 375	0.00011
$L.Cd^{II}$	265, 311, 366, 415	257, 389, 432	0.00035
$L.Pb^{II}$	281, 309, 395	248, 299, 398	0.00027
Emission			
H_2L	488	495	0.0031
$L.Cd^{II}$	578	603	0.0073
$L.Pb^{II}$	505	566	0.0064

REFERENCES

[S1] (a) H. A Benesi and J. H. Hildebrand, *J. Am. Chem. Soc*., 1949, **71**, 2703-2707; (b) A. Mallick and N. Chattopadhyay, *Photochem. Photobiol*., 2005, **81**, 419-424; (c) P. Roy, K. Dhara, M. Manassero, J. Ratha and P. Banerjee, *Inorg. Chem*., 2007, **46**, 6405-6412.

[S2] H. M. Irving, M. G. Miles and L. D. Pettit, *Anal. Chim. Acta*, 1967, **38**, 475-488.

[S3] L. Alderighi, P. Gans, A. Ienco, D. Peters, A. Sabatini and A. Vacca, *Coord. Chem. Rev*.. 1999, **184**, 311.